2D and 3D percolation in high-temperature superconductors

E. D. Specht, A. Goyal, and D. M. Kroeger
Oak Ridge National Laboratory, Oak Ridge, Tennessee 37831-6118
(Received 14 September 1995)

A quantitative model is presented for the high critical current densities (J_c) supported by superconducting materials with uniaxial alignment, such as *c*-axis textured Bi-Sr-Ca-Cu-O tapes. Current follows percolative paths across small-angle grain boundaries. Because j_c is low for intragranular conduction parallel to the *c* axis, the 3D flow required for percolation is produced by conduction perpendicular to the *c* axis in tilted grains. For optimized microstructures, J_c ranging from 3 to 30 % of the intragranular value is predicted for percolation across small-angle grain boundaries with misorientations below 10° and 20°, respectively.

I. INTRODUCTION

Long lengths of Bi-Sr-Ca-Cu-O superconducting tape have recently been fabricated with high J_c even in high magnetic fields. For the best samples, $J_c \sim 5\times10^4$ A/cm^2 both at temperature $T=77$ K in zero applied magnetic field B and at $T=4.2$ K, $B=20$ T. It is hoped that these materials will be useful for applications such as magnets and power transmission, once their properties are optimized.[1]

These tapes consist of a uniaxially aligned layer or layers of Bi-Sr-Ca-Cu-O within a silver sheath. The layers are composed of grains with a high aspect ratio: grain thickness H (normal to the tape surface) is ~1 μm, while length L and width W are ~20 μm (Fig. 1). The *c* axes of the grains are aligned normal to the films, with a distribution of $\sim15°$ full width at half maximum (FWHM), while the *a* axes are oriented randomly in the plane of the tape. We use these essential properties to model current transport. More detailed microstructural characterization and its implications for current transport are summarized by Bulaevskii *et al.*[2] What we refer to as ''grains'' are in fact ''colonies'' of grains joined by low-angle boundaries.

Despite broad agreement on the above description of Bi-Sr-Ca-Cu-O tapes, there is no consensus on the path followed by electrical current. The first model for the current path in *c*-axis-textured materials without in-plane alignment was the ''brick-wall'' model.[3,4] The brick-wall model is based on an ideal microstructure shown three dimensionally (3D) in Fig. 1 and in cross section in Fig. 2. The solid lines in Fig. 2 denote [001] tilt boundaries which we will call *ab* boundaries. The dashed lines are [001] twist boundaries which we call *c* boundaries. Both will typically be high angle. The brick-wall model assumes that the narrow *ab* boundaries carry negligible current. Although the *c* boundaries are high angle, their large cross-sectional area can support high currents in spite of low j_c. Hence current follows the path shown schematically by the fine line in Fig. 2, crossing *c* boundaries only. Such a current path requires intragranular conduction in the *c* direction. Because intragranular j_c is much smaller in the *c* direction than in the *ab* planes, it limits the critical current density in the brick-wall model.

However, measurements of the temperature dependence and anisotropy of J_c suggest that long-range current flow involves little or no *c*-axis conduction, thus casting doubt on the brick-wall mechanism.[5–8] Furthermore, cross sections of superconducting samples do not resemble the idealized brick wall of Fig. 2: few pure twist boundaries are observed. In addition, J_c measurements on Bi-Sr-Ca-Cu-O bicrystals show that most high-angle [001] twist boundaries do act as weak links.[9,10] These difficulties with the brick-wall model led to the development of the railway-switch model.[6,7]

According to the railway-switch model, current within grains flows only in *ab* planes: conduction in the *c* direction does not significantly contribute. Current is transported across the thickness of the sample by grains tilted with respect to the average texture. Current flows between grains across apparent small-angle tilt boundaries.[6,7]

A key premise of the railway-switch model is that the most frequently observed boundaries are small-angle [*hk*0] tilt boundaries, which Hensel, Grasso, and Flükiger call *c*-axis tilt boundaries. This conclusion is based on scanning

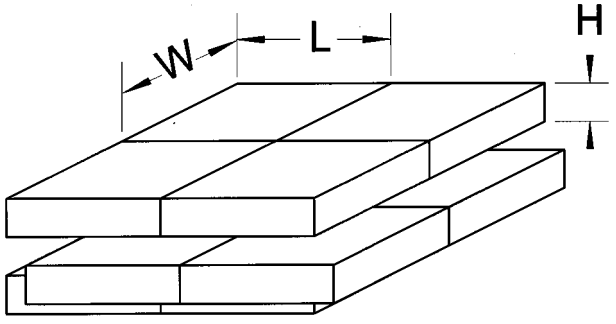

FIG. 1. Perspective view of a face-centered-tetragonal brick-wall microstructure. Each (001) plane forms a square lattice with primitive translations of $\pm\frac{1}{2},\frac{1}{2},0$.

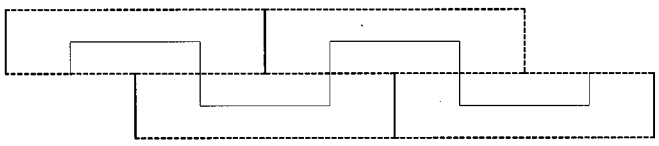

FIG. 2. Cross section of a brick-wall microstructure. Heavy solid lines: [001] tilt boundaries. Dashed lines: [001] twist boundaries. Fine solid line: current path in the brick-wall model.

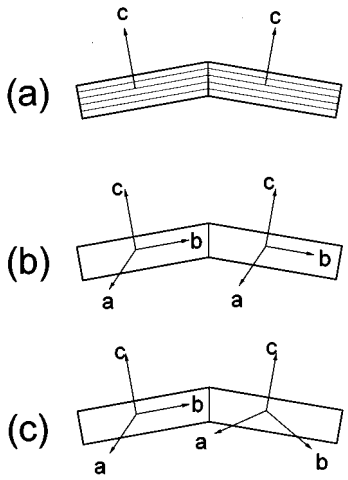

FIG. 3. (a) A cross section of the most commonly seen boundary shows only the $[hk0]$ tilt component. (b) the boundary may in fact be a low-angle $[hk0]$ tilt boundary, (c) but it is more likely to have a large [001] tilt component.

electron micrographs of cross sections of superconducting tapes.[7] We believe this conclusion is based on a misinterpretation of these micrographs. Many boundaries are observed which appear in cross section to be low-angle $[hk0]$ tilt boundaries, as shown schematically in Fig. 3(a). However, the micrographs give no indication of the [001] tilt component of such a boundary. While some are in fact low-angle boundaries [Fig. 3(b)], most are close to high-angle [001] tilt boundaries [Fig. 3(c)].

Little data has been published concerning j_c of grain boundaries in high-temperature superconductors as a function of grain-boundary character. The few published studies indicate that j_c for small-angle grain boundaries is close to intragranular j_c, while most high-angle grain boundaries act as weak links.[9,11–15] Reported values of the critical misorientation angle θ_c below which grain boundary j_c is high range from 10° to 20°.[12–15] Unfortunately, no estimate of θ_c is available for the Bi-Sr-Ca-Cu-O materials used in superconducting tapes.

Goyal *et al.* have characterized networks of small-angle grain boundaries in superconducting tapes and have proposed that long-range, strongly linked conduction occurs through a percolative network of small-angle grain boundaries.[16] Here we present a quantitative percolative model which explains how large J_c can be observed in materials in which only a small fraction f of the grain boundaries are small angle. We assume that j_c is large when grain-boundary misorientation is below θ_c of 10° to 20°, independent of other aspects of grain-boundary geometry: this is consistent with all available data. We further assume that all current flows in ab planes, as indicated by $J_c(B,T)$ at high B. Our percolative model has an ideal face-centered-tetragonal lattice of grains as shown in Figs. 1 and 2. While grains in real superconducting tapes are far from close packed,[7] we are most interested in the ultimate J_c which may be attained in superconducting tapes when the structure is optimized. As in the railway-switch model, tilted grains carry current in the n direction (normal to the tape's surface). Quantitative numerical results are presented for the percolation of current through a small fraction of grain boundaries which are small angle.

II. PERCOLATION AND DIMENSIONALITY

High total J_c can be carried by a material with a small fraction f of high j_c grain boundaries only when the sample combines the best aspects of 2D and 3D current flow. For a sample with perfect c-axis alignment, the maximum misorientation of a boundary between tetragonal grains is 45°. We assume that high-j_c boundaries require misorientations θ less than a critical angle θ_c of 10° to 20°. With a random orientation about the c axis, 22–44 % of grain boundaries have $\theta<10°$ to 20° (Fig. 5). Current flow, however, is strictly 2D, because there are no tilted grains to carry current normal to the sample thickness. In each ab plane of the model, the grains form a 2D square lattice, with a bond percolation threshold of 50%,[17] our model predicts that no current can percolate across a sample with perfect c-axis alignment. Even for the most favorable 2D case of a hexagonal lattice, the percolation threshold is 35%, so the material is near or below the percolation threshold and high J_c is not possible.

The situation is the opposite for unaligned material. Current flow is truly 3D, so percolation will occur when only 12% of the grain boundaries are conducting (for bond percolation on an fcc lattice).[18] However, only 3% of the grain boundaries have misorientations below θ_c of 20° (Fig. 5), so current cannot flow through low-angle boundaries in this limit either.

An optimum c-axis texture lies between these extremes. When the grains are slightly tilted, current is transported three dimensionally and large numbers of small-angle boundaries are present. Numerical calculations below demonstrate that large J_c can be supported in this manner.

III. CALCULATION OF J_c

As described above, a face-centered-tetragonal (fct) lattice of grains, shown in Figs. 1 and 2, is used to calculate J_c. Boundaries between grains separated by $\pm\frac{1}{2},\frac{1}{2},0$ translations (with respect to the fct lattice) are ab boundaries, with a {110} habit (with respect to the fct lattice). Boundaries between grains separated by $\pm\frac{1}{2},0,\frac{1}{2}$ translations are c boundaries, with a (001) habit. This describes a brick-wall microstructure.

Grains are assigned random orientations with the angle χ between their c axes and the sample normal n following a uniform distribution between 0° and $\chi_{\max}$, and no preferred orientation of the a and b axes.

Grain boundaries with misorientation greater than θ_c are nonconducting, i.e., $j_c=0$. A key assumption is that θ_c depends on misorientation only. Grain-boundary misorientation is the smallest angle of rotation between neighboring grain orientations. For tetragonal grain symmetry, misorientation angles fall between 0° and 45°.

For misorientations below θ_c, conduction is anisotropic, reflecting the c-axis texture of the material: critical current density j_c^{ab} for ab boundaries will be larger than j_c^c for c boundaries. Small-angle ab boundaries do not act as weak links, so they will have critical current density $j_c^{ab}=j_c^{\mathrm{SC}}$, the single-crystal value, and critical current $i_c^{ab}=HWj_c^{\mathrm{SC}}$, where

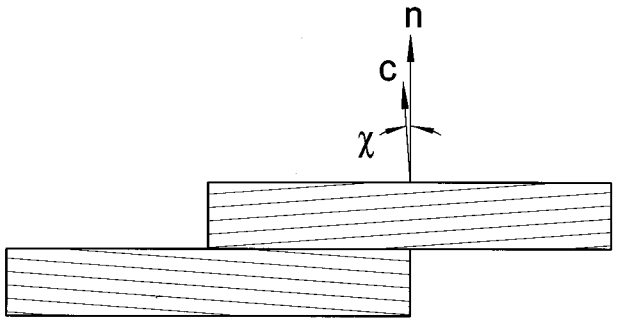

FIG. 4. The c axes superconducting grains make an angle χ to the sample normal n.

H and W are defined in Fig. 1.

Because current flows in ab planes, current flows parallel to the sample normal n only in grains where the c axis is tilted by a nonzero angle χ from the sample normal n (Fig. 4). This angle is taken to be uniformly distributed between 0° and $\chi_{\max}$, where the tetragonal crystal symmetry requires that $0°<\chi_{\max}<90°$. In real materials, both the c axes of the grains and the grain boundaries will be tilted; we have simplified the model by considering only c-axis tilts, leaving grain boundaries aligned to n.

Intragranular critical current density is j_c^{SC} flowing in the ab planes, so current density across strongly linked c boundaries is $j_c^{\mathrm{SC}}\sin\chi$. While we have calculated the fraction of strongly linked boundaries by assigning tilts to individual grains, we make the mean-field approximation that the critical current densities of all strongly linked c boundaries (i.e., those with $\theta<\theta_c$) are equal to the average value of the minimum critical current density of two neighboring grains. This was done to simplify calculations: the total J_c of the sample will depend on only three parameters, the fraction f of strongly linked boundaries, and the critical currents of ab and c boundaries. The average critical current density normal to a c boundary for a single grain is, for small $\chi_{\max}$,

$$\frac{j_c^{\mathrm{SC}}}{\chi_{\max}}\int_0^{\chi_{\max}} d\chi\,\sin(\chi)=j_c^{\mathrm{SC}}\left[1-\frac{\cos(\chi_{\max})}{\chi_{\max}}\right]\approx\frac{J_c^{\mathrm{SC}}\chi_{\max}}{2}, \tag{1}$$

and the average of the minimum value for two grains is

$$\frac{2j_c^{\mathrm{SC}}}{\chi_{\max}^2}\int_0^{\chi_{\max}} d\chi_1\int_0^{\chi_1} d\chi_2\,\sin(\chi_2)=\frac{2j_c^{\mathrm{SC}}}{\chi_{\max}^2}\left[\chi_{\max}-\sin(\chi_{\max})\right]$$
$$\approx\frac{j_c^{\mathrm{SC}}\chi_{\max}}{3}. \tag{2}$$

The area of c boundaries is $LW/4$, so the critical current normal to the c boundary is $i_c^c=LWJ_c^{\mathrm{SC}}\chi_{\max}/12$. For large aspect ratios, i_c^c would exceed HWj_c^{SC}, which is the critical current of the grain itself. In this case, i_c^c is truncated to HWj_c^{SC}. Results are normalized so that a sample with perfect biaxial alignment (i.e., a c-aligned single crystal) has a total $I_c=1$:

$$i_c^{ab}=\frac{1}{N^2};\quad i_c^c=\frac{L}{H}\frac{\chi_{\max}}{12N^2}, \tag{3}$$

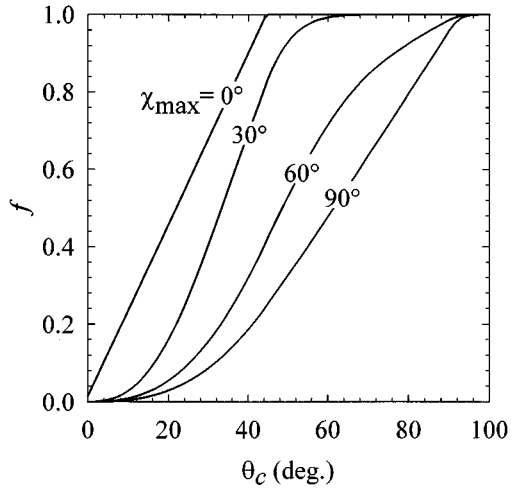

FIG. 5. Fraction f of grain boundaries with misorientation below θ_c for maximum tilt $\chi_{\max}$ calculated numerically using 10^6 randomly oriented pairs of grains for each value of $\chi_{\max}$.

where N^2 is the number of ab boundaries in a sample cross section. We take $L/H=20$.

Each grain boundary can carry currents between $-i_c$ and i_c [as given by Eq. (3)]. The total critical current I_c of the sample is calculated using the labeling method,[19] in which an exact solution is found by adding percolative paths until no conducting path can be added without exceeding the critical current of some boundary. Each grain forms a node on an fcc lattice. Each node is connected by 12 arcs (grain boundaries) to neighboring nodes.

I_c^{ab} (in the plane of the tape, as it is commonly measured) is calculated by applying periodic boundary conditions in the [010] and [001] directions (with respect to the fct lattice). The current source and sink are on the [100] faces. Infinite capacity is assumed within these faces, corresponding physically to good contacts covering each end of the sample. I_c^c (across the thickness of the tape) is similarly calculated by applying periodic boundary conditions in the [100] and [010] directions and placing the source, sink, and contacts on [001] faces. Note that I_c^{ab} flows across a cross section N^2HW, while the cross section for I_c^c is N^2LW, larger by a factor of $LH=20$. Thus $J_c^{ab}/J_c^c=20I_c^{ab}/I_c^c$.

The labeling algorithm is most efficient near and below the percolation threshold, where there are few percolative paths. Since this is the case where the largest sample size is required to obtain accurate results, sample size is varied to keep calculation time roughly constant, varying between a $14\times14\times14$ lattice with 65 856 grain boundaries below the percolation threshold to a $5\times5\times5$ lattice with 3000 grain boundaries well above the percolation threshold.

IV. RESULTS

For each combination of $\chi_{\max}$ and θ_c, the fraction f of grain boundaries with misorientations below θ_c is calculated by examining 10^6 randomly generated boundaries.[20] Selected results are shown in Fig. 5. I_c is calculated from f and i_c. We calculate i_c using Eq. (3). Figure 6 illustrates the relationship between I_c and f for several values of the grain-boundary critical current anisotropy i_c^c/i_c^{ab}.

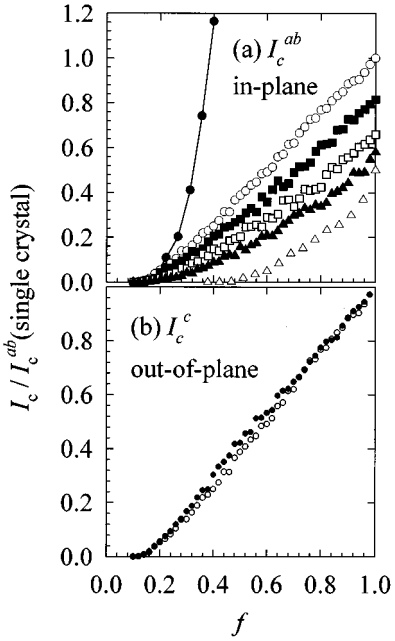

FIG. 6. Total (a) in-plane and (b) out-of-plane critical current as a function of the fraction of conducting grain boundaries for a variety of anisotropies in grain-boundary critical current: $i_c^{ab}=\infty$ and $i_c^c=1$ (●), the 3D case $i_c^{ab}=1$ and $i_c^c=1$ (○), $i_c^{ab}=1$ and $i_c^c=0.63$ (■), $i_c^{ab}=1$ and $i_c^c=0.32$ (□), $i_c^{ab}=1$ and $i_c^c=0.16$ (▲), and the 2D case $i_c^{ab}=1$ and $i_c^c=0$ (△). In each case, $i_c=1$ corresponds to the single crystal in-plane value.

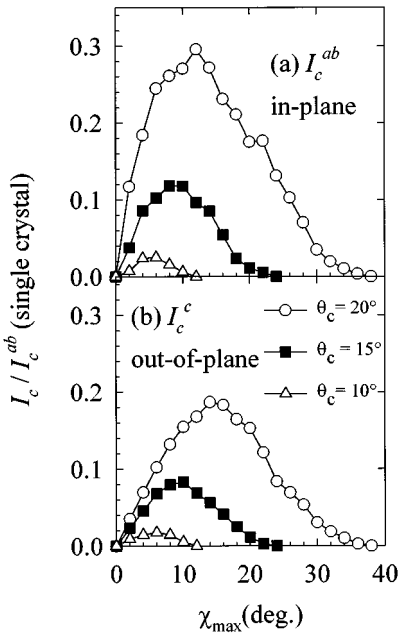

FIG. 7. Total (a) in-plane and (b) out-of-plane critical current, normalized to single-crystal values, as a function of maximum tilt for the experimentally observed range of critical misorientation values.

Random scatter in Fig. 6 is due to statistical variations in the calculation of I_c due to finite simulation size. For I_c^{ab}, these fluctuations become large for anisotropies less than 0.1. Results are obtained for these values by multiplying the result for $i_c^{ab}=\infty$ and $i_c^c=1$ by the value of i_c^c. Accurate values for $i_c^{ab}=\infty$ and $i_c^c=1$ were obtained by running calculations on a $14\times14\times14$ lattice. This calculation is time consuming, but must be performed only once for each value of f. Note that Fig. 6(a) includes two sets of points for the limit $i_c^{ab}\gg i_c^c$. In this limit, i_c is zero for conducting fraction $f<0.12$ (the 3D fcc bond percolation threshold), proportional to i_c^c [filled circles, Fig. 6(a)] for $0.12<f<0.5$ (the 2D square bond percolation threshold), when weak c boundaries couple ab planes which are themselves below the percolation threshold, and proportional to i_c^{ab} [open triangles, Fig. 6(a)] for $0.5<f<1$, when current can flow without crossing weak c boundaries. As f approaches 0.5 from below, i_c diverges to ∞ times i_c^c [filled circles, Fig. 6(a)]; as f approaches 0.5 from above, i_c approaches 0 times i_c^{ab} [open triangles, Fig. 6(a)].

I_c^c depends only weakly on i_c^{ab}. As shown in Fig. 6(b), there is at most a 20% difference between I_c^c for $i_c^{ab}=1$ and $i_c^c=1$ [open circles, Fig. 6(b)] and I_c^c for $i_c^{ab}=\infty$ and $i_c^c=1$ [closed circles, Fig. 6(b)]. For this reason, we can make the approximation $I_c\approx i_c^{ab}\ I_c(i_c^{ab}=1,\ i_c^c=1)$. Although I_c^c depends primarily on i_c^c, note that i_c^c depends on intragranular j_c^{ab}, because our percolation model neglects intragranular j_c^c.

I_c, normalized to single crystal I_c^{ab}, is shown in Fig. 7. The maximum I_c^{ab} is sensitive to θ_c, increasing a factor of 10 from 3 to 30 % as θ_c is doubled from 10° to 20°. This is because the material is close to the threshold for percolation of current through ab boundaries with high j_c, and a small change in θ_c, and thus in f, makes a large change in the number of c boundaries with low j_c needed for current to traverse the sample.

The optimum χ_{max} varies proportionately to θ_c from 5° to 10°. I_c will vary proportionately with the grain aspect ratio L/H as well, finally saturating when 3D percolation is reached at $L/H=12/\sin(\chi_{max})$ or 70 to 140.

I_c^c varies much as I_c^{ab}. This is to be expected, since our model predicts conduction by a 3D percolation mechanism. For small θ_c, f is far below the 2D percolation threshold of 0.50, so percolation is very isotropic and $I_c^c\approx I_c^{ab}$. For $\theta_c=10°$ and $\chi_{max}=8°$, for example, $I_c^{ab}/I_c^c=1.1$. As noted above, the ratio of total critical current densities will be $J_c^{ab}/J_c^c=22$. For larger θ_c, f is closer to the 2D percolation threshold, percolation is more anisotropic, and $I_c^c<I_c^{ab}$. For $\theta_c=20°$ and $\chi_{max}=8°$, for example, $I_c^{ab}/I_c^c=2.0$ and $J_c^{ab}/J_c^c=40$.

V. DISCUSSION

The I_c predicted by the percolative model are higher than those observed in Bi-Sr-Ca-Cu-O tapes. The percolative model predicts 3–30 % of single crystal I_c, depending most on θ_c for an ideal structure. The best tapes have $J_c\sim5\times10^4$ A/cm^2 ($T=77$ K, $B=0$), or ~0.5% of single crystal J_c. As pointed out by Hensel,[7] existing tapes contain numerous gaps between grains, so it is to be expected that substantial increases in J_c will result from the production of a more closely packed microstructure. The optimum χ_{max} of 5° to 10° is consistent with the 15° FWHM typically observed in optimized tapes. A better check of the percolative model calculation will require measurement of θ_c for Bi-Sr-Ca-Cu-O materials, as well as production of more closely packed tapes.

The measurement of J_c^c remains an experimental challenge. While the critical current I_c^c has been measured,[5,7] the critical current density J_c^c has not been reported. Such measurements will test our prediction that J_c^{ab}/J_c^c is 20–40 for the percolative model.

A key distinction between the percolative model and the brick-wall model is that I_c for the percolative model falls to zero as c-axis texturing is reduced below its optimum value of 5° to 10°. According to the brick-wall model, I_c should remain high for even the best-aligned samples. A test of this prediction will require production of Bi-Sr-Ca-Cu-O films with excellent c-axis alignment ($<2°$ FWHM) and no in-plane alignment. According to the percolative model, significant current in such films cannot flow through a network of strongly linked grain boundaries, and high J_c cannot be produced in strong applied magnetic fields.

In common with other models, the percolative model predicts that I_c will increase as the aspect ratio of grains increases. Further experimental data is required to check a key premise of the percolative model, that grain boundaries are weak links unless total misorientation is small, and conversely that all small-angle boundaries act as strong links.

The calculations presented here are best-case predictions because they assume a perfect lattice of grains. In real materials there will always be some gaps separating grains, so real J_c can only approach these values. 3D percolation requires $f>12\%$; for $\chi_{\max}=0°$ (which maximizes f), f ranges from 22% ($\theta_c=10°$) to 44% ($\theta_c=20°$). Thus a minimum of 27–55 % of the grain boundaries must be connected for strongly linked conductivity to occur.

The assumption that only small-angle grain boundaries can have high critical currents may be unduly pessimistic, however. Some large-angle [001] twist boundaries have been found with J_c as large as the intragranular value.[9] Note, however, that intragranular J_c for these boundaries is in the c direction and is therefore limited to low values. Large-angle grain boundaries with truly high J_c have not been observed. A final possibility for J_c greater than predicted by the percolative model is that low-angle boundaries may occur with greater frequency than dictated by chance alone; i.e., local orientational order may occur.[16]

ACKNOWLEDGMENTS

We have benefited from helpful discussions with G. E. Ice. This research was sponsored by the U.S. Department of Energy, Assistant Secretary for Conservation and Renewable Energy, Office of Utility Technologies, Office of Management/Advanced Utility Concepts—Superconducting Technologies for Electric Energy Systems and Division of Materials Sciences under Contract No. DE-AC05-84OR21400 with Lockheed Martin Energy Systems.

[1] P. Majewski, Adv. Mater. **6**, 593 (1994).
[2] L. N. Bulaevskii, L. L. Daemen, M. P. Maley, and J. Y. Coulter, Phys. Rev. B **48**, 13 798 (1993).
[3] A. P. Malozemoff, in *Superconductivity and its Applications*, edited by Y. H. Kao, A. E. Kaloyeros, and H. S. Kwok, AIP Conf. Proc. No. 251 (AIP, New York, 1992), p. 6.
[4] L. N. Bulaevskii, J. R. Clem, L. I. Glazman, and A. P. Malozemoff, Phys. Rev. B **45**, 2545 (1992).
[5] J. H. Cho, M. P. Maley, J. O. Willis, J. Y. Coulter, L. N. Bulaevskii, P. Haldar, and L. R. Motowidlo, Appl. Phys. Lett. **64**, 3030 (1994).
[6] B. Hensel, J.-C. Grivel, A. Jeremie, A. Perin, A. Pollini, and R. Flükiger, Physica C **205**, 329 (1993).
[7] B. Hensel, G. Grasso, and R. Flükiger, Phys. Rev. B **51**, 15 456 (1995).
[8] A. Umezawa *et al.*, Physica C **219**, 378 (1994).
[9] J.-L. Wang, X. Y. Cai, R. J. Kelley, M. D. Vaudin, S. E. Babcock, and D. C. Larbalestier, Physica C **230**, 189 (1994).
[10] N. Tomita, H. Takahashi, M. Mori, and Y. Ishia, Jpn. J. Appl. Phys. **31**, L942 (1992).
[11] S. E. Babcock and D. C. Larbalestier, J. Phys. Chem. Solids **55**, 1125 (1994).
[12] D. Dimos, P. Chaudhari, J. Mannhart, and F. K. LeGoues, Phys. Rev. Lett. **61**, 219 (1988).
[13] D. Dimos, P. Chaudhari, and J. Mannhart, Phys. Rev. B **41**, 4038 (1990).
[14] E. Sarnelli, P. Chaudhari, W. Y. Lee, and E. Esposito, Appl. Phys. Lett. **65**, 362 (1994).
[15] T. Nabatame, S. Koike, O. B. Hyun, I. Hirabayashi, H. Suhara, and K. Nakamura, Appl. Phys. Lett. **65**, 776 (1994).
[16] A. Goyal, E. D. Specht, D. M. Kroeger, T. A. Mason, D. J. Dingley, G. N. Riley, and M. W. Rupich, Appl. Phys. Lett. **66**, 2903 (1995).
[17] M. F. Sykes, D. S. Gaunt, and M. Glen, J. Phys. A **9**, 97 (1976).
[18] M. F. Sykes and J. W. Essam, Phys. Rev. **133**, A310 (1964).
[19] L. R. J. Ford and D. R. Fulkerson, *Flows in Networks* (Princeton University Press, Princeton, New Jersey, 1962), p. 17.
[20] A. Goyal, E. D. Specht, and D. M. Kroeger (unpublished).